An Ultrasensitive Colorimetric Strategy for Detection of Cadmium Based on the Peroxidase-like Activity of G-Quadruplex-Cd(II) Specific Aptamer

Bin ZHOU,*† Ya-Ting CHEN, Xin-Yi YANG,** Yong-Sheng WANG,** Xi-Jiang HU,* and Qing-Li SUO*†**

**Wuhan Children's Hospital (Wuhan Maternal and Child Healthcare Hospital), Tongji Medical College, Huazhong University of Science & Technology, 100 Hong Kong Road, Jiang'an District, Wuhan City, Hubei Province 430016, China*

***College of Public Health, University of South China, 28 Chang sheng West Road, Hengyang City, Hunan Province 421001, China*

We rationally designed an ultrasensitive and label-free sensing platform for determination of cadmium (Cd). The sensing platform contains G-quadruplex-Cd(II) specific aptamer (GCDSA) constructed by incorporating G-rich sequence at the end of 5′ and the critical domain of the Cd-4 aptamer. GCDSA designed act as both a special recognition sequence for Cd^{2+} and a signal DNAzyme. In absence of Cd^{2+}, GCDSA may mainly exist in a random coil sequence. Upon addition of Cd^{2+}, GCDSA could probably be induced to fold into a G-quadruplex structure. The generation of plentiful active G-quadruplex interacts with hemin to form a peroxidase-like DNAzyme, leading to increased absorbance signal of the sensing system. ΔA was directly proportional to the two segments of concentrations for Cd^{2+}, with the detection of limit of 0.15 nM. The proposed method avoids the labeled oligonucleotides and allows directly quantitative analysis of the samples by cheap instruments, with an excellent dynamic range.

Keywords Cd(II)-specific aptamer, cadmium, G-quadruplex, absorbance, conformation switching

(Received May 30, 2018; Accepted October 23, 2018; Advance Publication Released Online by J-STAGE November 2, 2018)

Introduction

Cadmium (Cd) is classified as a prevalent toxic heavy metal, and it is used widely in the manufacture of nick-cadmium batteries and production of pigments, paints, alloys and solar panels. China is the largest manufacturer of cadmium and accounts for almost 30% of world cadmium consumption in 2012.[1] Cadmium emission into environment through waste gas, water, and residue has gradually observed due to the increased consumption. For example, high degree of Cd pollution in the riverine sediments of the Haihe Basin and Longjiang River in China has been reported.[2,3] Cd concentrations in rice of some areas were also excessive to the criteria regulated by the Ministry of Health of the People's Republic of China (0.2 mg/kg).[4] Polluted soil area with 20 million hm^2 accounts for about 20 percentage of the Chinese area.[5] Long-term exposure to low concentrations of Cd by soil-rice-human chain model is toxic to certain organisms, such as kidney,[6,7] liver[8] and lung,[9] with biological half-life in the range of 10 – 30 years.[10] Therefore, the quantification of Cd has become increasingly important in environmental and food samples.

The efficient analytical techniques for determination of Cd have been widely reported, such as atomic fluorescence spectrometry (AFS),[11-13] inductively coupled plasma mass spectrometry (ICP-MS),[14,15] atomic absorption spectroscopy (CVG-AAS)[16-18] and high performance liquid chromatography.[19] Although the above mentioned techniques are accurate and efficient, many of them either require costly equipment or skilled operators.

DNAzyme, RNAzyme or aptamer are functional nucleic acids, which possesses highly affinity and precise molecular recognition capabilities for a vast range of targets.[20,21] Most functional nucleic acids strongly rely on metal ions, thus they have been extensively used to detect metal ions in optical and electrochemical sensors.[22-24] Researchers have reported a DNA aptamer for Cd determination,[25] which can specifically bind to Cd^{2+} with high affinity and stability. An electrochemical sensor based on aptamer is used for detection of Cd^{2+}, and the detection is fast and aptasensor can be reused.[26]

G-quadruplex as the most of famous structure of DNA, are G-rich nucleic acid sequences[27] and stabilized by hydrogen bonds and alkali metal ions, which are located in the center between two G-quartets.[28] Meanwhile, the structure of G-quadruplex relys on the composition and length of the DNA, on the orientation of the chains and positions of the loops, and also on the nature of the cations.[29] G-quadruplex DNAzymes are peroxidase-like complexes based on covalent attachment of hemin moiety to the G-quadruplex scaffold,[30] which has widely drawn the attention of researchers for a decade. Many kinds of G-quadruplexes DNAzymes as sensing probes have been intensively applied to various analytical methods of targets,

B. Z. and Q.-L. S. equally contributed to this work.
† To whom correspondence should be addressed.
E-mail: zhoubin19860528@126.com

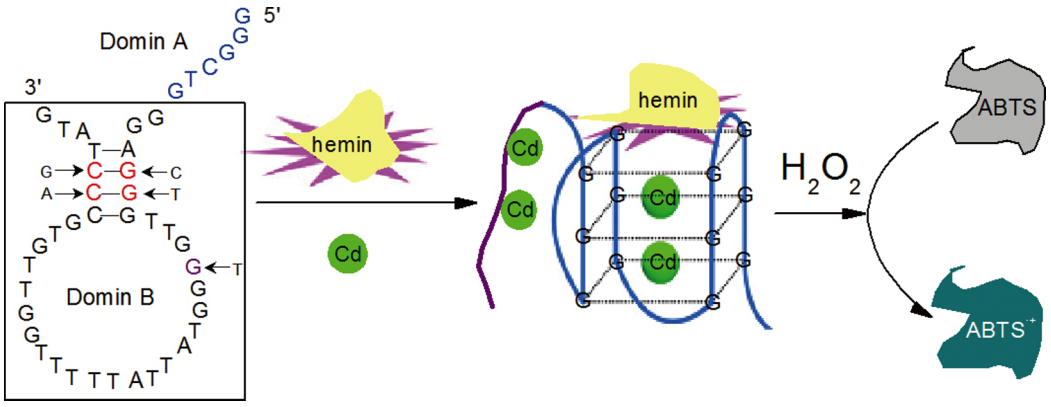

Scheme 1 Schematic diagram of a novel singly label-free assay for Cd^{2+}.

such as Cu^{2+},[31] Pb^{2+},[32] Hg^{2+},[33,34] Mg^{2+} [35] and Sr^{2+}.[36,37] Recently, our group reported a dual-channel detection of metallothioneins and mercury based on the flexible G-quadruplex.[38] The related researches on colorimetric strategy for detection of certain heavy metal ions (*e.g.*, Hg^{2+}, Cu^{2+}, Pb^{2+}, Ag^{+}) have also been reported.[39–43] As far as we know that there is no report on the determination of Cd using the specific G-quadruplex by colorimetric strategy.

This work focuses on establishing an ultrasensitive and cost-effective sensor for the accurate and quantitative determination of Cd^{2+}. G-quadruplex-Cd(II) specific aptamer (GCDSA) is a functional DNA probes. Cd^{2+} could induce conformational switching of the GCDSA probe to strengthen the peroxidase-like activity of G-quadruplex DNAzymes, which leads to a remarkable increase of absorbance signal.

Experimental

Reagents and chemicals

The oligonnucleotide strands, Mes buffer, hemin and 2,2′-azinobis(3-ethylbenzothiozoline)-6-sulfonic acid (ABTS) were supplied by Sangon Biotech Co., Ltd. (Shanghai, China). The used DNA sequences were given in follow:

GCDSA: 5′-GGGCTGGGAGGGTTGGGGTATTATTTTTGG-TTGTGCCCTATG-3′;

Complementary strands: 5′-CCCAACCCT-3′ (9 bases); 5′-CCCAACCCTCC-3′ (11 bases).

DNA concentrations were represented as single-stranded concentrations, which were determined by measuring the absorbance at 260 nm. The final concentrations of hemin and ABTS were 2 μM and 5 mM, respectively, which were stored in freezer far from light. All chemicals in the experiment were analytical grade. Deionized water (18.2 MΩ cm resistivity) was used in this work.

Apparatus

Shimadzu UV-2550 spectrophotometer (Kyoto, Japan) was utilized to collect the UV-vis absorption spectra of the system with quartz cuvette.

Assay for Cd^{2+}

Fifty mM Tris–HCl buffer was prepared to 2-mL EP tube, and then 30 μL of the GCDSA solution (1 μM) and the different concentration of Cd^{2+} was added to this solution, and the mixture were incubated for 30 min. Thereafter, 70 μL of 2 mM hemin was added to the mixture and kept for another 60 min. Ninety microliters of 50 mM-H_2O_2 and 50 μL of 5 mM-ABTS were added to the above solution, followed by adding an appropriate amount of water to a volume of 500 μL. After standing for 15 min, the UV-vis absorption spectra were measured at λ_{max} 416 nm, and quantified by $\Delta A = A_1 - A_0$, where A_0 and A_1 were the absorbance of the system without and with Cd^{2+}, respectively.

Results and Discussion

GCDSA design and Cd^{2+}-triggering signal change detection

We rationally designed an ultrasensitive and label-free sensing platform for the determination of cadmium (Cd). As illustrated in Scheme 1, the sensing platform included Cd^{2+}, hemin, H_2O_2, 2,2-azino-bis(3-ethylbenzothiazoline)-6-sulfonicacid (ABTS) and GCDSA. GCDSA with a 42-mer oligoncleotide was a novel peroxidase-like functional aptamer, and it is designed based on the critical domain of the Cd-4 aptamer[25] (marked with a black line in Scheme 1). The critical domain of Cd-4 aptamer can fold into stem-loop structure, and the loop may provide sufficient binding sites for Cd^{2+} through the coordination bonds between Cd^{2+} and the adjacent short fragment rich in T or G[25]. In our previous research, we also constructed multifunctional Cd(II)-specific aptamer *via* extending of two G bases in the 5′ terminal and labeling a 6-FAM in the 3′ terminal based on the critical domain of Cd-4 aptamer.[44] The 5′ terminal of the critical domain of Cd-4 aptamer contains densely six G bases, then we replaced the C, T, G and A bases with two G bases and two C bases in the stems section (the red fonts in Scheme 1), which still contained 4 pairs of bases, and replaced a T base with G bases on the loop (the purple fonts in Scheme 1). Furthermore, we extended 6 bases including 4 G bases at the 5′ end (the blue fonts in Scheme 1). Thus, the base sequence designed becomes G-rich sequence, which contains three G bases separated by short stretches of other bases and also basically retained the base of the loop binding site. G-rich sequences can potentially self-associate into stacks of G-quartets to form complex structural motifs known as G-quadruplexes.[45] At the same time, we used a web-based server, the QGRS Mapper, to predict the potential formation of intramolecular G-quadruplexes directly from GCDSA.[46] In QGRS parameters, x is 3, $y1$ is 1, $y2$ is 2, indicating that the sequence of GCDSA contain three tetrads ($x > 2$). The DNA structure with three or more G-tetrads was considered to be more stable and meant to form quarplexes.[47,48] Data view in the QGRS Mapper showed that the highest G-score

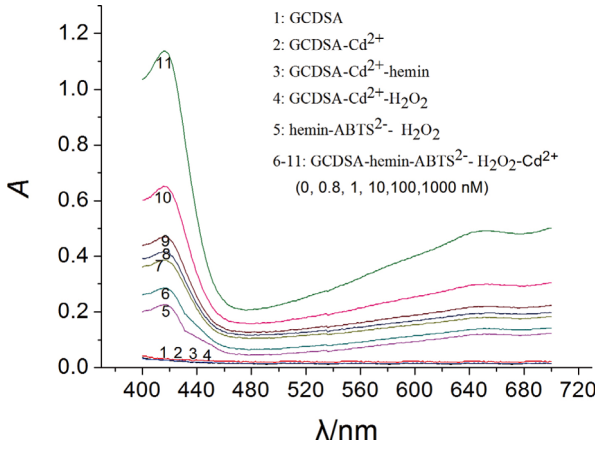

Fig. 1 Absorption spectra of the Cd^{2+}-hemin-ABTS-H_2O_2 system. (1) GCDSA; (2) GCDSA-Cd^{2+}; (3) GCDSA-Cd^{2+}-hemin; (4) GCDSA-Cd^{2+}-H_2O_2; (5) hemin-ABTS-H_2O_2; (6 – 11) GCDSA-hemin-ABTS-H_2O_2-Cd^{2+} ($C_{Cd^{2+}6\text{-}11}$ = 0, 0.8, 1, 10, 100, 1000 nM) C_{ABTS} = 5 mmol L^{-1}, C_{H2O2} = 0.1 mmol L^{-1}.

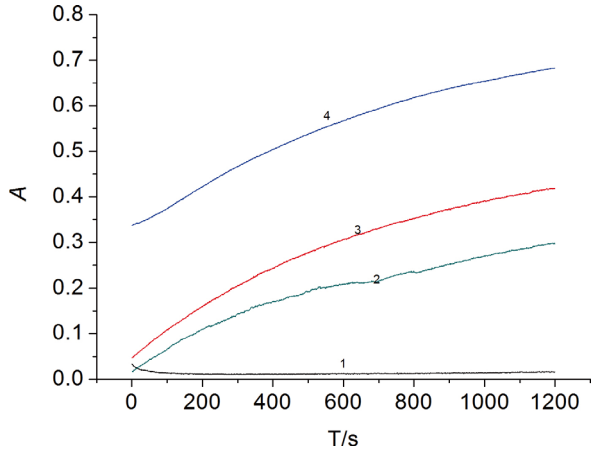

Fig. 2 Catalytic activity of the GCDSA-Cd^{2+}-$ABTS^{2-}$-H_2O_2 system. $C_{Tris\text{-}HCl}$ = 15 mmol L^{-1}, C_{DNA} = 0.06 μmol L^{-1}, C_{Hemin} = 0.28 mmol L^{-1}, C_{ABTS} = 0.5 mmol L^{-1}, C_{H2O2} = 1.6 mmol L^{-1}, $C_{Cd^{2+}} = 6 \times 10^{-7}$ mol L^{-1}.

is 41 (Table S1, Supporting Information). So, the GCDSA may form the G-quadruplex. In a word, GCDSA consists of two regions on basis of different functions. Domain A was constructed by G (Guanine)-rich sequence, and Domain B was the critical domain of the Cd-4 aptamer.[25] So, GCDSA could function as both a special recognition sequence for Cd^{2+} and a peroxidase-like DNAzyme for signal generation. In the absence of Cd^{2+}, GCDSA may mainly exist in a random coil sequence. The G-quadruplex-forming sequences were initially limited, in this case, the low absorbance intensity can be expected, then with addition of Cd^{2+} into hemin-H_2O_2-ABTS solution, and Cd^{2+} could probably promoted the GCDSA to fold into an active G-quadruplex structure. The generation of massive active G-quadruplex interacts with hemin forming DNAzyme, which catalyzes the oxidation of ABTS by H_2O_2, resulting in the color change of solution and significantly enhanced absorbance intensity of the sensing system for sensitive monitoring of Cd^{2+}.

Spectral characteristics

As mentioned above, we inferred that Cd^{2+} might manipulate the structure switching of GCDSA to forming the activity of G-quadruplex DNAzyme. To confirm the presumption, the absorption spectra of the GCDSA-Cd^{2+}-$ABTS^{2-}$-H_2O_2 system was obtained. As shown in Fig. 1, the aqueous solutions of GCDSA (curve 1), GCDSA-Cd^{2+} (curve 2), GCDSA-Cd^{2+}-hemin (curve 3) and GCDSA-Cd^{2+}-H_2O_2 (curve 4) showed almost no absorption signal, and the hemin in H_2O_2-$ABTS^{2-}$ system exhibited a low absorption peak at the round of 416 nm (curve 5). Upon addition of GCDSA, a relative increased absorption intensity was observed (curve 6), which implied that GCDSA was likely to form the low activity of DNAzyme. The addition of Cd^{2+} into the solution of GCDSA-hemin-H_2O_2-$ABTS^{2-}$ (curve 7 to curve 11), Cd^{2+} induced a remarkable enhanced absorption intensity and accompanied by a visible color deepened, which indicated that Cd^{2+} probably could overwhelmingly facilitate to form massive active G-quadruplex, resulting in a noticeable enhanced catalytic activity on the oxidation of ABTS by H_2O_2. So, the series of data support our hypothesis.

Figure 2 shows the catalytic activity of the GCDSA-Cd^{2+}-$ABTS^{2-}$-H_2O_2 system. The $ABTS^{2-}$-H_2O_2 solution (curve 1) showed almost no catalytic activity and the hemin-$ABTS^{2-}$-H_2O_2 (curve 2) had a slow reaction velocity, then with the addition of GCDSA, the absorbance value of the solution was a small increase (curve 3), indicating that the oxidation of $ABTS^{2-}$ started slowly. Upon addition of Cd^{2+}, the signal of absorption intensity increased rapidly (curve 4), leading to the accumulation of the colored radical product ($ABTS^{\cdot+}$), which may be the formation of massive G-quadruplex with the high activity of DNAzyme. The serial of data was in accordance with our presumption and the above design as shown in Scheme 1.

Selection of complementary chains paired with Cd(II) specific aptamer

Given that our detection system in absence of Cd^{2+} has a low catalytic activity of G-quardruplex DNAzymes, which results in the absorbance value of 0.4 at the 416 nm in blank group. So, we attempted to design two kinds of complementary chains paired with Guanine-rich sequence of the GCDSA (one is nine bases and another is eleven bases) to reduce absorbance value of blank group. The interesting results are shown as Fig. S1(A) (Supporting Information), with addition of 9 bases or 11 bases complementary strands, the absorbance value in blank group was decline from 0.4 to 0.2 or 0.15 (curve 1), indicating that the complementary strand may effectively paired with GCDSA and greatly inhibited the formation of G-quadruplex in blank group. While in our experiment group with a mount of Cd^{2+}, the absorbance value was changed from 0.9 to 0.7 or 0.55 (curve 2). It meant that the ΔA decreased along with complementary strands of 9 or 11 bases. So, complementary chain was not chosen for the determination of Cd^{2+}.

Influence of the concentration of hemin, H_2O_2, ABTS and GCDSA

The concentrations of hemin, H_2O_2 and ABTS must be optimized for the sensitivity of assay. The concentration of H_2O_2 was evaluated from 2 to 10 mmol L^{-1}. As can be shown in Fig. S1(B), the ΔA was significantly increased along with the concentrations of H_2O_2 from 2 to 9 mmol L^{-1}, and sharply decreased from 9 to 10 mmol L^{-1}. Thus, 9 mmol L^{-1} of H_2O_2 was chosen for the highest analytical signals. Then, the concentrations of ABTS and GCDSA were evaluated from 0.1 to 0.8 mmol L^{-1} and from 10 to 80 nM, respectively. Figures S1(C) and S1(D) accordingly show the results of ABTS and GCDSA concentrations optimized, during the GCDSA-catalyzed oxidation process, along with the increasing ABTS

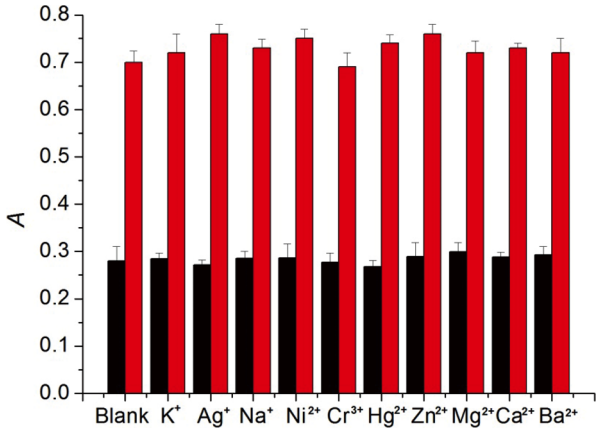

Fig. 3 Selectivity of the Cd^{2+} determination system. Blank black bars represent the absorption value at 416 nm of system in absence of Cd^{2+} and foreign substances; the other black bars represent the absorption value at 416 nm of system in the presence of other metal ions (10 μM); blank red bars represent the absorption value at 416 nm of system only in present of Cd^{2+}; the other red bars represent the absorption signals of the sensing systems in presence of Cd^{2+} (C = 141 nM) and other metal ions.

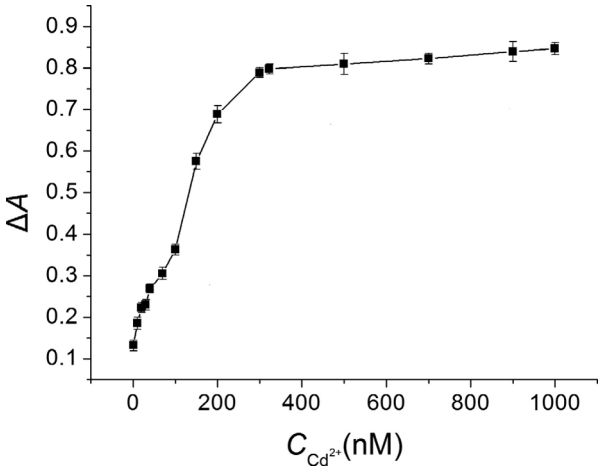

Fig. 4 Calibration curve of colorimetric strategy for Cd^{2+}.

Table 1 A comparison of the characteristics reported in the previous papers and the present study

Detection limit	Linear range	Analytical method	Ref.
0.008 μg L^{-1}	0.03 – 500 μg L^{-1}	CVG-AFS[a]	10
0.02 μg L^{-1}	0.02 – 25 μg L^{-1}	HG-AFS[b]	11
0.19 μg L^{-1}	0.63 – 500 μg L^{-1}	CVG-AFS	12
0.0022 μg L^{-1}	—	MSPME-ICP-MS[c]	13
3.9 ng L^{-1}	—	ICP-MS	14
0.16 μg L^{-1}	0.5 – 30 μg L^{-1}	VSLLME-SFO-FAAS[d]	15
1.1 μg L^{-1}	—	FAAS	16
5.0 pg	16.7 – 1000 pg	GFAAS[e]	17
—	—	HPLC-ICP-MS	18
0.017 μg L^{-1} (0.15 nM)	0.056 – 22.48 μg L^{-1} 33.72 – 112.41 μg L^{-1}	Colorimetric strategy	Our work

a. Chemical vapor generation system coupled with atomic fluorescence spectrometry.
b. Hydride generation atomic fluorescence spectrometry.
c. Magnetic solid phase microextraction combined with inductively coupled plasma mass spectrometry.
d. Vortex-assisted surfactant-enhanced-emulsification liquid-liquid microextraction with solidification of floating organic droplet combined with flame atomic absorption spectrometry.
e. Graphite furnace atomic absorption spectrometry.

concentrations. The ΔA increased at the beginning and sharply reached a maximum at the 0.5 mmol L^{-1}, then gradually decreased. So, the concentration of ABTS was accurately controlled in 0.5 mmol L^{-1}. In Fig. S1(D), the ΔA of system gradually increased along with further addition of GCDSA from 5 to 10 μL, then decreased from 10 to 20 μL, again significantly increased from 20 to 30 μL, and the ΔA exhibited maximum value when the GCDSA concentration was 30 μL, which would be propitious to the subsequent quantitative determination for Cd^{2+}. Therefore, 30 μL was chosen as the optimized volume in the experiment.

Sensitivity and selectivity of determination system

To study the selectivity of determination system, the likely interference ions in the assay were tested, including K^+, Ag^+, Na^+, Ni^{2+}, Cr^{3+}, Hg^{2+}, Zn^{2+}, Mg^{2+}, Ca^{2+} and Ba^{2+}. Figure 3 demonstrates that Cd^{2+} (141 nM) and one of other metal ions (10 μM) could significantly increase the absorbance intensity with Cd^{2+} alone. By comparison, no obvious changes were observed upon the addition of other metal ions (10 μM). These may be attributed to the structural differences between Cd^{2+}-stabilized G-quadruplexes and other metal ions-stabilized G-quardruplexes.[49] Zhou reported the G-quadruplex-hemin DNAzyme for Ag^+ determination, showing a high selectivity over a range of other metal ions.[50] These indicate that a highly sensitive and selective strategy for Cd^{2+} is achieved in the presence of other metal ions.

Figure 4 demonstrates the favorable wide quantification range used to determine the concentration of Cd^{2+}. It is noteworthy that in the target concentrations range of 0.5 – 323 nM, the regression equation is expressed as $\Delta A = 0.002C(\text{nM}) + 0.162$ with a correlation coefficient of 0.962, and in the target concentrations range of 323 – 1000 nM, the regression equation is expressed as $\Delta A = 0.00005C$ (nM) + 0.769 with a correlation coefficient of 0.988. The limit of detection (LOD) for the determination of Cd^{2+} in our method was 0.15 nM. A comparison of the characteristics reported in the previous papers and the present study is given in Table 1. The results suggest that Cd^{2+}-sensing platform can be applied for the extremely low concentration of Cd^{2+} quantitation.

Compared with previous sensing method,[26,44] the proposed one has several obvious advantages. GCDSA is a label-free functional oligonucleotides probe, which greatly reduces the cost of bioassay and complexity of working mechanism. The detection signal can be judged by simple spectrophotometer, eliminating the use of expensive instruments. Furthermore, the whole detection method is very simple and ultrasensitive, thus avoiding the demands for skilled performers in analysis of extremely low concentrations of samples.

Application of Cd^{2+} ion detection assay in real samples

At last, the potential application of our proposed colorimetric platform was evaluated by the environmental samples from tap water, the pond water in University of south China and Xiangjiang river. The all samples were filtered through a 0.22-μm membrane, then we divided them into two samples.

Table 2 Determination results of Cd^{2+} in the environmental samples (n = 6)

Sample	Method	Found/ nM	Added/ nM	Total found	RSD, %	Recovery, %	t
1[a]	Colorimetric	—	50.00	51.32	2.30	102.64	1.58
	FL	—	50.00	50.72	1.58	101.44	
2[b]	Colorimetric	—	50.00	52.50	3.01	105.00	2.01
	FL	—	50.00	51.34	2.34	102.68	
3[c]	Colorimetric	—	50.00	49.60	1.44	99.20	1.67
	FL	—	50.00	51.32	2.56	102.64	

Theoretical t (5, 95%) = 2.571.
a. Xiangjiang river water.
b. Tap water.
c. Pond water in University of South China.

One is added to the HEPES buffer of pH 7.3 for determination by the previous fluorospectrophotometry.[44] Another was determined by our work according the procedure described above. The quantitative results are described in Table 2. The t values acquired by colorimetric and fluorescent strategys[44] do not exceed the theoretical value. We can see a good performance in analysis of environmental samples.

Conclusions

In summary, we designed a functional GCDSA probe to develop the excellent assay for determination of Cd^{2+}. In the experiment only one label-free GCDSA oligonucleotides was demanded, which was manipulated to form massive active G-quadruplex-hemin DNAzyme by a quantity of Cd^{2+}. The unique and "turn on" working design for Cd^{2+} determination can reduce the testing cost and simplify the experiment procedure, and the proposed sensing method exhibits the two segment of wide linear range, allowing the detection limit of Cd^{2+} at concentrations as low as 0.15 nM.

Acknowledgements

This work is subsidized by the National Natural Science Foundation of China (No. 81502850), the Natural Science Foundation of Hunan Province in China (No. 2015JJ2122) and Undergraduate inquiry learning and innovative experimental project in Hunan province (No. 336).

Supporting Information

This material is available free of charge on the Web at http://www.jsac.or.jp/analsci/.

References

1. Merchant Research & Consulting Ltd, "*Cadimum: Global Market Trends and Prospects to 2027*", **2014**, Market Publishers Ltd., London
2. W. Tang, W. Zhang, Y. Zhao, H. Zhang, and B. Shan, *Ecol. Indic.*, **2017**, *81*, 295.
3. X. M. Zhao, L. A. Yao, Q. L. Ma, G. J. Zhou, L. Wang, Q. L. Fang, and Z. C. Xu, *Chemosphere*, **2018**, *194*, 107.
4. W. Ji, Z. Chen, D. Li, and W. Ni, *Energy Procedia*, **2012**, *16*, 27.
5. J. Yan, G. Quan, and C. Ding, *Procedia Environ. Sci.*, **2013**, *18*, 78.
6. L. Shi, H. Cao, J. Luo, P. Liu, T. Wang, G. Hu, and C. Zhang, *Ecotoxicol. Environ. Saf.*, **2017**, *145*, 24.
7. L. Barregard, G. Bergström, and B. Fagerberg, *Environ. Res.*, **2014**, *135*, 311.
8. M. Mikowska and R. Świergosz-Kowalewska, *Chemosphere*, **2018**, *199*, 625.
9. X. Zeng, X. Xu, H. M. Boezen, J. M. Vonk, W. Wu, and X. Huo, *Environ. Pollut.*, **2017**, *230*, 838.
10. W. M. L. Shan, Y. B. Yi, Z. Y. Zhou, and F. Le, *PLoS One*, **2014**, *9*, 1.
11. X. A. Yang, M. B. Chi, Q. Q. Wang, and W. B. Zhang, *Anal Chim. Acta*, **2015**, *869*, 11.
12. H. Yu, X. Ai, K. Xu, C. Zheng, and X. Hou, *Analyst*, **2016**, *141*, 1512.
13. R. Sun, G. Ma, X. Duan, and J. Sun, *Spectrochim. Acta, Part B*, **2018**, *141*, 22.
14. X. Yu, B. Chen, M. He, H. Wang, and B. Hu, *Talanta*, **2018**, *179*, 279.
15. R. S. Amais, A. Virgilio, D. Schiavo, and J. A. Nóbrega, *Microchem. J.*, **2015**, *120*, 64.
16. G. Peng, Y. Lu, Q. He, D. Mmereki, X. Tang, Z. Zhong, and X. Zhao, *Water Sci. Technol.*, **2016**, *73*, 2781.
17. A. T. Duarte, M. B. Dessuy, M. G. R. Vale, B. Welz, and J. B. de Andrade, *Talanta*, **2013**, *115*, 55.
18. H. Tinas, N. Ozbek, and S. Akman, *Microchem. J.*, **2018**, *138*, 316.
19. V. Devesa and D. Vélez, in "*Encyclopedia of Food and Health*", **2016**, Academic Press, Oxford, DOI: https://doi.org/10.1016/B978-0-12-384947-2.00096-9, 543.
20. J. Huang, X. Su, and Z. Li, *Biosens. Bioelectron.*, **2017**, *96*, 127.
21. L. Mo, J. Li, Q. Liu, L. Qiu, and W. Tan, *Biosens. Bioelectron.*, **2017**, *89*, 20.
22. I. Palchetti and F. Bettazzi, in "*Reference Module in Chemistry*", **2017**, Molecular Sciences and Chemical Engineering, Elsevier, DOI: https://doi.org /10.1016/ B978-0-12-409547-0.
23. L. Mo, J. Li, Q. Liu, L. Qiu, and W. Tan, *Biosens. Bioelectron.*, **2017**, *89*, 201.
24. J. Huang, X. Su, and Z. Li, *Biosens. Bioelectron.*, **2017**, *96*, 127.
25. Y. Wu, S. Zhan, L. Wang, and P. Zhou, *Analyst*, **2014**, *139*, 1550.
26. H. R. Lotfi Zadeh Zhad, Y. M. Rodríguez Torres, and R. Y. Lai, *J. Electroanal. Chem.*, **2017**, *803*, 89.
27. C. K. Kwok and C. J. Merrick, *Trends Biotechnol*, **2017**, *35*, 997.
28. T. Fujii, P. Podbevšek, J. Plavec, and N. Sugimoto, *J. Inorg Biochem.*, **2017**, *166*, 190.
29. D. L. Ma, H. Z. He, K. H. Leung, H. J. Zhong, D. S. Chan, and C. H. Leung, *Chem. Soc. Rev.*, **2013**, *42*, 3427.
30. J. Kosman, A. Stanislawska, A. Gluszynska, and B. Juskowiak, *Int. J. Biol. Macromol.*, **2017**, *101*, 799.
31. Y. Wang, Y. Wu, W. Liu, L. Chu, Z. Liao, W. Guo, G.-Q. Liu, X. He, and K. Wang, *Talanta*, **2018**, *178*, 491.
32. H. Sun, L. Yu, H. Chen, J. Xiang, X. Zhang, Y. Shi, Q. Yang, A. Guan, Q. Li, and Y. Tang, *Talanta*, **2015**, *136*, 210.
33. J. Ge, X. P. Li, J. H. Jiang, and R. Q. Yu, *Talanta*, **2014**, *122*, 85.
34. M. Liu, Z. Wang, L. Pan, Y. Cui, and Y. Liu, *Biosens. Bioelectron.*, **2015**, *69*, 142.

35. Y. Y. Yan, J. Lin, T. M. Ou, J. H. Tan, D. Li, L. Q. Gu, and Z. S. Huang, *Biochem. Biophys. Res. Commum.*, **2010**, *402*, 614.
36. A. C. Fyfe, P. W. Dunten, M. M. Martick, and W. G. Scott, *J. Mol. Biol.*, **2015**, *427*, 2205.
37. I. M. Pedroso, L. F. Duarte, G. Yanez, A. M. Baker, and T. M. Fletcher, *Biochem Biophys. Res, Commun.*, **2007**, *358*, 298.
38. X. Tang, Y. S. Wang, J. H. Xue, B. Zhou, J. X. Cao, S. H. Chen, M. H. Li, X. F. Wang, Y. F. Zhu, and Y. Q. Huang, *J. Pharm. Biomed. Anal.*, **2015**, *107*, 258.
39. Y. Ding, S. Wang, J. Li, and L. Chen, *TrAC, Trends Anal. Chem.*, **2016**, *82*, 175.
40. Z. Zhang, H. Wang, Z. Chen, X. Wang, J. Choo, and L. Chen, *Biosens. Bioelectron.*, **2018**, *114*, 52.
41. L. Chen and J. Li, *ACS Appl. Mater. Interfaces*, **2014**, *6*, 15897.
42. L. Chen, X. Fu, W. Lu, and L. Chen, *ACS Appl. Mater. Interfaces*, **2013**, *5*, 284.
43. T. Lou, Z. Chen, Y. Wang, and L. Chen, *ACS Appl. Mater. Interfaces*, **2011**, *3*, 1568.
44. Y. F. Zhu, Y. S. Wang, B. Zhou, J. H. Yu, L. L. Peng, Y. Q. Huang, X. J. Li, S. H. Chen, X. Tang and X. F. Wang, *Anal. Bioanal. Chem.*, **2017**, *409*, 4951.
45. K. K. Chun and J. M. Catherine, *Trends Biotechnol.*, **2017**, *35*, 997.
46. K. Nucleic, A. Lawrence, and S. B. Paramjeet, *Nucleic Acids Res.*, **2006**, *34*, W676.
47. M. I. Zarudnaya, I. M. Kolomiets, A. L. Potyahaylo, and D. M. Hovorun, *Nucleic Acids Res.*, **2003**, *31*, 1375.
48. B. I. Kankia, G. Barany, and K. Musier-Forsyth, *Nucleic Acids Res.*, **2005**, *33*, 4395.
49. H. Sun, X. Li, Y. Li, L. Fan, and H. B. Kraatz, *Analyst*, **2013**, *138*, 856.
50. X. H. Zhou, D. M. Kong, and H. X. Shen, *Anal. Chim. Acta*, **2010**, *678*, 124.